Performance Evaluation of a Solid-State Detector Based Handheld Gamma Camera System

Peter Knoll*[1], S. Mirzaei[1], K. Schwenkenbecher[2], T. Barthel[2]

1. Department of Nuclear Medicine and PET Center, Austria
2. Crystal Photonics GmbH, Germany

Article info:
Received: August 3 2013
Accepted: October 17 2013

Keywords:
Handheld gamma camera,
Solid state detector,
Radiopharmaceutical guided surgery.

ABSTRACT

Purpose: In this work we present a handheld, solid-state detector based gamma camera system. We validated the camera physically and demonstrated the usefulness of the device for intra-operative detection of radiolabeled tissue.

Methods: We measured the intrinsic uniformity, the intrinsic energy resolution, the system uniformity, the spatial resolution without scatter, the system planar uniformity, the detector shielding and the peak deviation according to the NEMA NU1-2001 standard.

Results: The gamma camera can be used for isotopes with an energy range between 50-250 keV. A standard laptop is used to control of the camera and to visualize Preliminary clinical data show that the devices can be used successfully for a number of clinical applications.

Conclusion: The performance evaluation of a novel handheld gamma camera shows good spatial resolution, sensitivity and energy resolution. Due to the small size and weight the portable device can be used for untraoperative acquisitions.

1. Introduction

Gamma cameras are used by physicians to measure the distribution of radiolabeled substances within the human body. Several technical improvements in developing imaging devices for nuclear medicine have been shown in the last decades. In the very first attempts to measure radionuclide distributions an array of radiation detectors has been used [1]. Later, rectilinear scanners were used to scan a rasterlike pattern around the area of a patient [1]. The major disadvantages of sequential imaging were solved by the introduction of a scintillation gamma camera by Hal Anger [2]. The Anger gamma camera consists of a scintillation crystal, a number of photomultiplier tubes and an electronic position logic circuit. The energy of the γ-ray is absorbed by the crystal and converted into visible photons. For detection these photons have to leave the crystal and photomultiplier tubes are used to convert the photons into individual electronic pulses (indirect conversion). The sum of the pulses is applied to determine the energy signal, and the position of the event in the crystal.

This basic concept of the gamma camera design has not changed in the last decades. The recent use of solid state detectors might change the landscape of gamma cameras since it improves the energy, spatial resolution and contrast of these imaging systems through direct conversion of the energy and location of the detected photon into an electronic pulse [3, 4]. Thus, applying solid state detectors direct conversion scheme, the gamma-ray is converted into an electric pulse providing both the energy and the location of the event [5]. First gamma cameras, equipped with a solid state detector are already commercially available. Comparison of these new developed cameras with standard NaI-detector gamma cameras shows an improved energy, spatial resolution and count sensitivity [3].

*** Corresponding Author:**
Peter Knoll, PhD
Department of Nuclear Medicine and PET Center, Wilhelminenspital, Montleartstr. 37, 1171 Vienna, Austria.
Tel: +43 1 49150 5771
E-mail: peter.knoll@wienkav.at

However, one of the main advantages of such a system is the possibility to realize different concepts to develop gamma camera systems. For example, in sentinel node detection nowadays scintillation probes are used to measure the radioactive uptake in the first draining lymph node. This methodology is used in the staging of several cancers in the operating room to identify the sentinel lymph node (SLN) which should be removed, it is one of the most important prognostic signs. The detection with standard gamma cameras is also possible, but they lack the opportunity for intraoperative localisation. The clinical need to improve detection and to observe in real-time if the lesion is correctly removed, leads to small, handheld gamma cameras [6]. In this work we describe the use of a novel solid state detector handheld gamma camera. We present acceptance test measurements according to the NEMA NU1-2001 standard for performance measurements of scintillation cameras [7], the successful use for very first patient measurements and the possible use of this system for preclinical imaging.

2. Methods

2.1. Operation Principles and Technical Properties

The handheld gamma camera (CrystalCam, Crystal Photonics GmbH, Berlin, Germany) used in this study has a square shape with 65 mm side length and 180 mm length, and a total weight of 800 g (Figure 1). The sides of the camera are shielded with 3 mm lead. The device is optimized for the most common nuclide in nuclear medicine, ^{99m}Tc, which emits gamma rays of 140 keV but can be used for energies from 50-250 keV. The gamma camera is equipped with a standard laptop on which the control and visualization software is installed. Collected events are continuously transmitted to the laptop via a USB port. All necessary voltages, including the high voltage (-600 V) for the detector, are generated in the gamma camera from the 5V provided by the USB-port. The time resolution of the system ranges from 0.1 -600 seconds.

2.2. Detector

The handheld camera detection unit is based on a cadmium-zinc-telluride (CdZnTe, CZT) semiconductor with dimensions of 40 × 40 × 5 mm. On the CZT crystal a continuous metal contact on the cathode side and a pixelated metal contact on the anode side are applied. The detection matrix consists of 16 x 16 pixels (256 pixels) on which application-specific integrated circuits (ASICs) are mounted. Each pixel has an area of 1.86 × 1.86 mm and the pixel pitch is 2.46 mm. When a gamma photon hits the detector, electron-hole pairs are generated. Under the influence of the electric field, the electrons and holes drift to their corresponding electrode. The resulting pulse is measured and digitized by the ASICs. The number of generated charge carriers is proportional to the energy of the incident gamma photon. Each event is tagged with a pixel number, an energy channel (0 – 4095) and a time stamp.

The event information is transferred from the detector to the microcontroller board using the serial peripheral interface (SPI) protocol [8]. The microcontroller board carries all components to control the detection unit and to transfer data to and from the host laptop, respectively. All communications between the gamma camera and the host laptop are handled through USB. The microcontroller board also carries the high voltage supply,

Figure 1. Handheld gamma camera

which uses the 5V input provided by USB and generates -600V for the detector

To obtain the energy information of the incident gamma photon in keV a calibration for each pixel needs to be made. Since the channel-to-energy dependence is linear, one can measure two different nuclides to obtain offset and gain values for each pixel which are stored in the laptop. The standard energy range of the gamma camera is 40 – 250 keV.

2.3. Collimator Design

Four different collimators are available for the handheld gamma camera (Figure 2). Each collimator has a matched design, which means that each collimator hole fits precisely a detector pixel and has therefore 256 holes.

The open field collimator has no collimation and is appropriate for homogeneity calibration and quality control measurements. It also serves as transport protection.

The low energy high resolution (LEHR) collimator is a parallel- square-hole collimator with 2.16×2.16 mm hole size and 0.3 mm septa. The length is 22.58 mm. The LEHR collimator is designed for high spatial resolution. Therefore it is suitable especially for applications where the separation of very close objects is important, e.g. sentinel lymph nodes in the maxillofacial region.

The low energy high sensitivity (LEHS) collimator is a parallel- square-hole collimator with 2.04×2.04 mm hole size and 0.42 mm septa. The length is 11.15 mm. The LEHS collimator is designed for very high sensitivity and is especially suitable for applications where the objects have very low activities, e.g. sentinel lymph nodes in case of melanoma. The medium energy general purpose (MEGP) collimator is a parallel-circular-hole collimator with 1.5 mm hole diameter and 0.96 mm septa and the length is 11.5 mm.

The collimators can be changed at runtime and are automatically detected by the gamma camera and the software application.

2.4. Calibration

Prior to the measurement, a calibration of the imaging system needs to be performed. After performing a measurement for intrinsic calibration, system calibration was done for each collimator using the flat field calibration phantom (Figure 3) filled with 10 MBq ^{99m}Tc. For the calibration 30 Mill- cts were acquired.

2.5. Camera Performance Measurements

Not only Camera Performance evaluation was done according to the NEMA NU1-2001 standard [7] but also vendor specific test was applied to ensure image quality. In detail, measurements to determine intrinsic uniformity, intrinsic spatial resolution, intrinsic energy resolution, system flood field uniformity, system spatial resolution without scatter, system planar sensitivity, and detector shielding were performed.

Due to the small field-of-view (FOV) no differentiation for the central- and useful FOV was made.

The peak deviation test, a vendor specific procedure, compares the measured photo peak with the theoretical photo peak value of the corresponding nuclide, e.g. ^{99m}Tc (140 keV).

The software attempts to automatically find the energy position of the photo peak of the measured nuclide by using a weighted derivation of each pixel's spectrum. Afterwards the user can verify the peak positions and correct them if necessary. The software then displays the relative deviation from the peak found and the nuclide's theoretical photo peak energy.

The acquired data of all measurements were analysed by vendor and self-developed softwares.

2.6. Clinical Data

The sentinel lymph node (SLN) is defined as the first lymph node that drains the primary tumor basin. The SLN can be mapped by using a sulphur-colloid radiotracer labeled with ^{99m}Tc that is injected near the primary tumor. Approximately 18- 37 MBq of tracer is injected near the primary tumor, with up 74 kBq of activity accumulating in the sentinel lymph nodes after it drains through the lymphatic channel [9]. Till now 17 patients were imaged using the novel handheld gamma camera system.

The handheld gamma camera can also be used for preclinical imaging with a special positioning adapter (Figure 4). Here, the animal is put on top of the imaging device.

3. Results

3.1. Intrinsic Uniformity

This measurement was performed by using the open field collimator using 15 MBq ^{99m}Tc which was filled in the flat field calibration phantom. The acquisition was done using a symmetric 15% photopeak window and 1.024 Mill cts. The calculation of the integral and differential uniformity was performed by vendor specific software. The results are shown in Table 1.

Table 1. Intrinisc uniformity measurements

Integral uniformity	3.2%
Differential uniformity	1.8%

3.2. Intrinsic Energy Resolution

The measurement of the intrinsic energy resolution was done by using the flat field calibration phantom that was filled with 15 MBq ^{99m}Tc. The calculations for each pixel using vendor specific software are shown in Figure 5.

The mean value of the energy resolution for each pixel is 5.2%.

3.3. System Uniformity

Here the flat field calibration phantom was filled with ^{99m}Tc using an energy window of 15% centered on the photopeak. The measurements were done using the three available collimators.

The calculation of the integral and differential uniformity was done by the vendor software (Table 2).

Table 2. System uniformity measured for various collimators

Collimator Type	Integral [%]	Differential[%]
LEHR	5.8	3.8
MEGP	5.3	3.5
LEHS	5.3	3.0

3.4. System Spatial Resolution without Scatter

The system spatial resolution was measured for each of the three collimators by positioning a blood gas capillary tube (diameter 1.75 mm) directly on the collimator surface. The measurements were done in x- and y- direction. Afterwards the full width at half maximum (FWHM) and full width at tenth maximum (FWTM) of the line spread function was calculated according to the NEMA NU1 standard [7]. The results of this measurement are shown in Table 3. Additional measurement was done by using the LEHR collimator (Table 4) and varying the distance from the capillary tube and the detector surface (0, 2.5 and 5 cm).

Table 3. System resolution without scatter: 0 mm distance, various collimators

Collimator Type	Distance 0 cm			
	FWHM [mm]		FWTM [mm]	
	x-direction	y-direction	x-direction	y-direction
LEHR	1.93	2.03	3.49	3.66
MEGP	1.91	1.89	3.46	3.42
LEHS	2.27	2.98	5.17	7.74

Table 4. System resolution without scatter: various distances, LEHR collimator

Distance from the Detector	FWHM [mm]		FWTM [mm]	
	x-direction	y-direction	x-direction	y-direction
0.0 cm	1.93	2.03	3.50	3.66
2.5 cm	3.74	3.89	6.88	8.07
5.0 cm	5.02	4.78	9.00	10.60

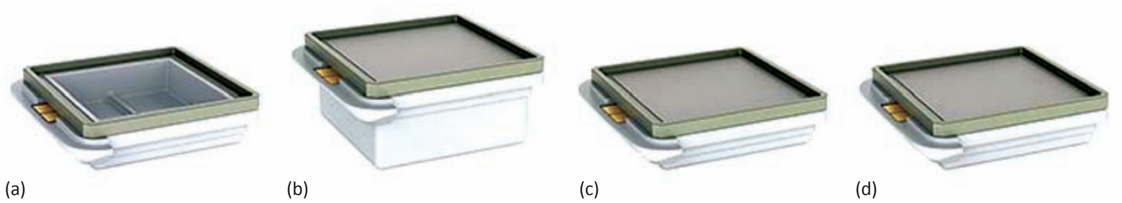

Figure 2. Changeable Collimators
a. Open field
b. Low Energy High resolution (LEHR)
c. Low Energy High sensitivity (LEHS)
d. Medium Energy General purpose (MEGP)

3.5. System Planar Sensitivity

The sensitivity measurements were done with 75 MBq ^{99m}Tc that were filled in a bottle. The analysis of the acquired data was done with a software tool provided by the acquisition software (Table 5).

Table 5. System planar sensitivity measured for various collimators

Collimator type	cpm/MBq
LEHR	14 220
MEGP	10 620
LEHS	33 240

3.6. Detector Shielding

Using the LEHR collimator the collimator count rate was measured with a ^{99m}Tc source (1000 MBq) was placed 10 cm in front of the collimator. Afterwards the source was moved around the sides of the detector to find the location of maximum counts. To calculate the shield leakage this value is divided by the collimator count rate and multiplied by 100.

The shield leakage value of the handheld gamma camera device was determined 5.78%

3.7. Peak Deviation

The maximum peak deviation was measured with the flat field calibration phantom which was filled with 50 MBq ^{99m}Tc. The result of this measurement was 3%.

3.8. Patient Studies

In 17 patients who were scheduled for sentinel node biopsy (7m and 5f with melanoma and 5f with breast cancer) imaging of the SLN was performed using the handheld gamma camera. The imaging were performed 20-60 minutes post peritumoral injection of 18 MBq of ^{99m}Tc human serum albumin colloids (Senti-Scint®, MEDI-Radiopharma, Budapest, Hungary) [10]. Representative images obtained by conventional planar gamma camera and the novel handheld gamma camera show similar results (Figure 6).

4. Discussion

In this work we present a small, portable gamma camera with a solid–state detector (CdZnTe, CZT) for accurate real-time visualization and localization of lesions (Figure 1). As mentioned previously, CZT has a high density and therefore a high efficiency to stop gamma rays effectively [11]. Since the detector material is a semiconductor, direct conversion of the gamma-ray leads to an electrical impulse. four different collimators are available to use the possible energy range of the device (40-250 keV) and different clinical applications. The measured data are visualised using a laptop computer. Due to the device's light weight, the portable use of the camera is possible. This allows for example the use of the imaging device in the operation room to control the result of the surgical procedure.

Intra-operative imaging is useful for detection of radio-labeled lesions at clinical activity levels, because it allows to efficiently discriminate nodes from ducts [11].

Furthermore, for the comfortable probing of small animals an acrylic specimen platform was developed (Figure 4). Our measurements according to the NEMA NU1-2001 standard [7] indicate that the basic performance, such as energy resolution, system resolution and sensitivity of this camera is favourable with the existing Anger gamma camera technology. The measurement of

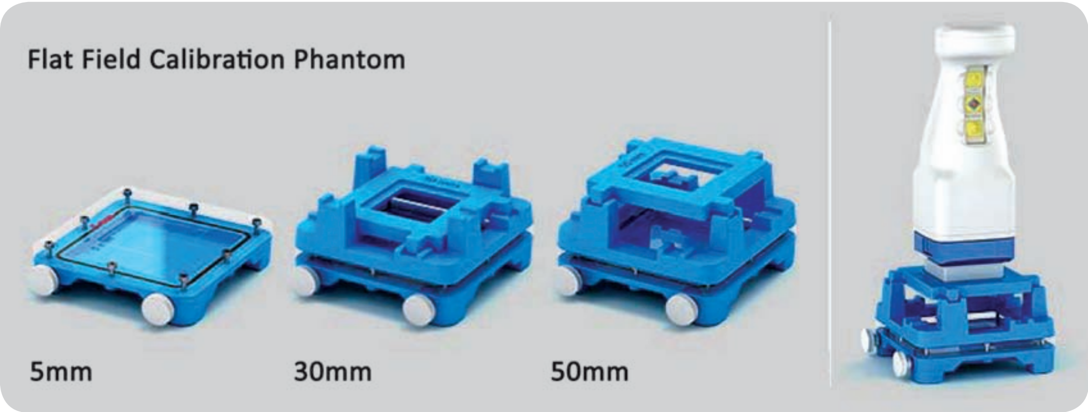

Figure 3. Flat field calibration phantom

Figure 4. Animal platform

a ^{99m}Tc line source, positioned directly on the collimator surface, shows for the low-energy high resolution collimator (LEHR) FWHM values of 1.93 mm in x-direction, 2.03 in y- direction (Table 3). The measurement of the system sensitivity shows 33 240 cpm/MBq (Table 5). The shield leakage of the handheld device was 5.7%. The improvement in sensitivity can be used for a dose reduction, in order to expose the patient to lower radiation [4].

The advantage of the presented system is the very low weight of 800 g, which allows easy handling of the system without the use of an articulated arm. The sentinel node detection is mainly used to locate the dissemination of lymph nodes in breast cancer and melanoma cases [13]. Several cases in which the radio-guided localization of sentinel lymph nodes is difficult with the bulky setup of a conventional gamma camera (e.g. due to the particular anatomical site) are reported in the literature [14]. The possibility of obtaining an intra operative image of the specimen could help to confirm whether the lesion is correctly removed [15].

The preliminary attempts to localise sentinel lymph nodes marked with ^{99m}Tc have been successful. The novel handheld gamma camera has been used to visualise the sentinel nodes in 17 patients almost immediately. Comparable results with a standard gamma camera are shown in Figure 6. Due to the high mobility of the system, the surgeon in the operating room has the possibility to observe and control the surgical procedure. One disadvantage of the system is, that the image quality might be altered by motion blurring [9]. The image quality can be improved by attaching the handheld gamma camera to an articulating arm [16]. However, the big advantage to conventional gamma cameras is not an improvement in image quality, but the higher sensitivity and flexibility due the portable design.

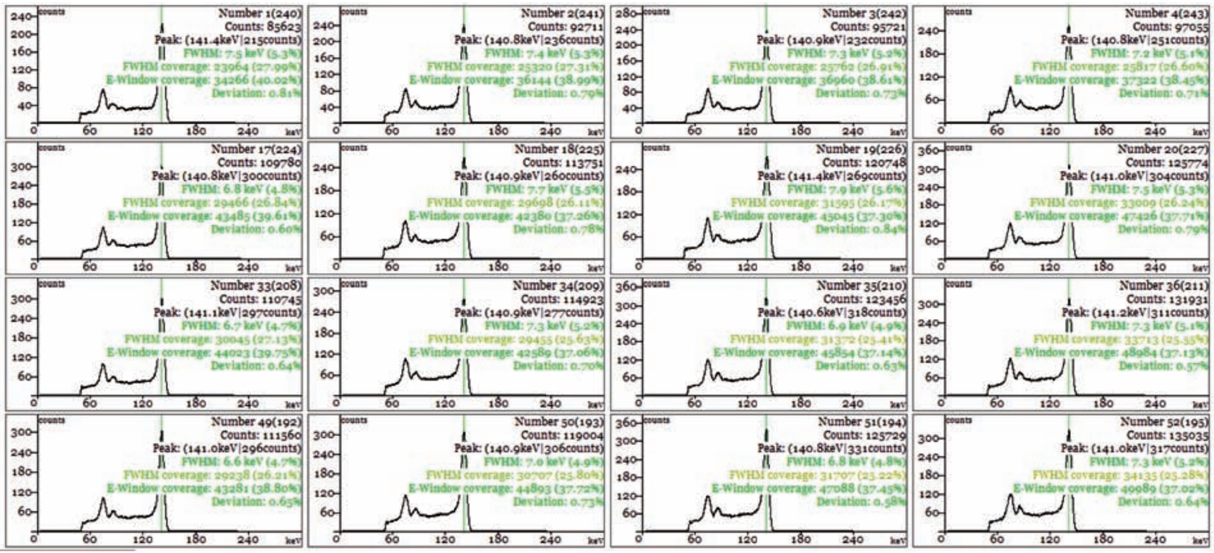

Figure 5. Energy spectrum measured for each pixel

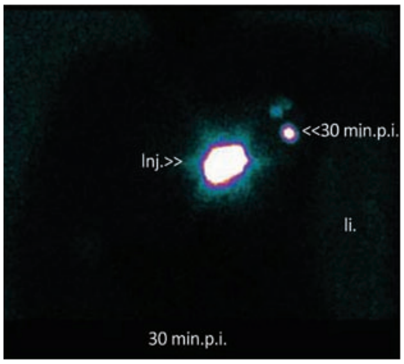

(a) (b)

Figure 6. Patient study:

a. Depot injection and sentinel node on a planar image acquired by conventional gamma camera

b. Visualisation of the sentinel node by handheld gamma camera

5. Conclusion

In this work we present the acceptance test and possible clinical use of a novel portable solid-state detector based portable gamma camera. Our preliminary results indicate that the device is useful for a number of clinical applications such as sentinel node detection and radioguided surgery.

Acknowledgments

The present study was supported by the SaveMe project, Project ID: 263307, as part of the Seventh Framework Programme, Theme 4 - NMP - Nanoscience, Nanotechnologies, Materials and New production.

References

[1] Sorenson, J.A., Phelps M.E. (1987). Physics in nuclear medicine. WB Saunders Company, Philadelphia .

[2] Anger, H.O. (1958). Scintillation camera. Rec Sci Instrum, 29, 27-33.

[3] Sharir, T., Slomka, P.J., Berman, D.S. (2010). Solid state SPECT technology: fast and furious. J Nucl Cardiol., 17(5), 890-6.

[4] Garcia, E.V., Faber, T.L. and Esteves, F.P. (2011). Cardiac dedicated ultrafast SPECT cameras: new designs and clinical applications. J Nucl Med, 52 (2), 210-7.

[5] Zanzionico, P., Heller, S. (2000). The intraoperative gamma probe: basic principles and choices available. Semin Nucl Med, 30, 33-48.

[6] Fernandez, M.M., Benlloch, J.M., Cerda, J., et al. (2004). A flat-panel-based mini gamma camera for lymph node studies. Nucl Instr. And Methods in Physics Research A, 527, 92-96.

[7] National Electrical Manufacturers Association. (2001). NEMA Standards Publications NU 2-2001: Performance Measurements of Positron Emission Tomography, Rosslyn, VA, USA.

[8] Serial peripheral interface (SPI). (2013). Can be find at: http://en.wikipedia.org/wiki/Serial_Peripheral_Interface_Bus

[9] Olcott, P.D., Habte, F., Foudray, A. et al. (2007). Performance Characterization of a minuature, high sensitivity gamma ray camera. IEEE Trans Nuclear Science, 54, 1492-1497.

[10] Mirzaei, S., Rodrigues, M., Hoffmann, B., et al. (2003). Sentinel lymph node detection with large human serum albumin colloid particles in breast cancer. European Journal of Nuclear Medicine and Molecular Imaging, 30(6), 874-8.

[11] Abe, A., Takahashi, N., Lee J. et al. (2003). Performance evaluation of a handheld semiconductor (CdZnTe)-based gamma camera. European Journal of Nuclear Medicine and Molecular Imaging, 30 (6), 805-11.

[12] Kopelman, D., Blevis, I., Iosilevsky, G., et al. (2005). A newly developed intr-operative gamma camera: performance charcteristics in a laboratory phantom study. European Journal of Nuclear Medicine and Molecular Imaging, 32 (19), 1271-24.

[13] Hsueh, E.C., Hansen, N., Guilano, A.E. (2000). Intraoperative lymphatic mapping and sentinel node detection in breast cancer. CA Cancer J Clin, 50 (5), 279-291.

[14] Russo, P., Mettivier, G., Pani, R. et. al. (2009). Imaging performance comparison between a LaBr3: Ce scintillator based and a CdTe semiconductor based photon counting compact gamma camera. Med. Phys, 36(4), 1298-317.

[15] Paredes, P., Vidal-Sicart, G., Zanon, G. et al. (2008). Radioguided occult lesion lkocalisation in breast cancer using intraoperative portable gamma camera: first results. European Journal of Nuclear Medicine and Molecular Imaging, 35(2), 230-5.

[16] Aasvold, J.N., Mintzer, R.A., Greene, C. et al. (2002). Gamma cameras for intraoperative localization of sentinel nodes: Technical requirements identified through operating room experience. 2002 IEEE Nuclear Science Symposium Conference Record, 2, 1172 - 1176.